Lattice instability and magnetic phase transitions in strongly correlated MnAs

Valeri Petkov[1,*], Adeel Zafar[1], Durga R. Tadisetti[1,2] and Milinda AM Abeykoon[3]

[1]*Department of Physics, Central Michigan University, Mt. Pleasant, Michigan 48858, USA*
[2]*Department of Physics, GITAM, Visakhapatnam, Andhra Pradesh 530045, India*
[3]*Photon Sciences Division, Brookhaven National Laboratory, Upton, New York 11973, USA*

Abstract

Using variable temperature x-ray total scattering in magnetic field, we study the interaction between lattice and magnetic degrees of freedom in MnAs, which loses its ferromagnetic order and hexagonal lattice symmetry at 318 K to recover the latter and become a true paramagnet when the temperature is increased to 400 K. Our results show that the 318 K transition is accompanied by highly anisotropic displacements of Mn atoms that appear as a lattice degree of freedom bridging the hexagonal and orthorhombic phases of MnAs. This is a rare example of a lowering of an average crystal symmetry due to an increased displacive disorder emerging on heating. Our results also show that magnetic and lattice degrees of freedom appear coupled but not necessarily equivalent control variables for triggering phase transitions in strongly correlated systems in general and in particular in MnAs.

E-mail: petko1vg@cmich.edu
*To whom correspondence should be addressed

1. Introduction

Strongly correlated systems exhibit unconventional properties due to the presence of interacting spin, charge, and lattice degrees of freedom [1-4]. A typical example is MnAs known to exhibit colossal magnetostriction, magnetoresistance, and magnetocaloric effects [5-10]. Upon heating, it undergoes a first-order transition at T_c = 318 K, where its ferromagnetic (FM) hexagonal ('H') structure transforms into an orthorhombic ('O') structure with zero net magnetization (see Figure 1). Concurrently, the atomic volume diminishes sharply. Such transitions are rare because, typically, the crystal symmetry of the higher-temperature phase appears higher than that of the low-temperature phase due to the usual increase in the symmetry of atomic displacements with temperature [11]. The transition temperature has been found to strongly depend on magnetic field. Moreover, it has been found that when the applied field exceeds a few T, the 'H' structure can be recovered via a first-order metamagnetic phase transition [12]. A second-order phase transition takes place at about 400 K, where the 'H' structure is recovered due to thermal excitations. The magnetic susceptibility above 400 K obeys the Curie-Weiss law, indicating that the high-temperature 'H'-phase is a true paramagnet. The magnetic response of the 'O'-phase, however, is strongly non-linear and the magnetic susceptibility exhibits a maximum at the second-order transition, suggesting that MnAs is an antiferromagnet (AF) in the temperature range from 318 K to 400 K [13].

The concurrent structural and magnetic phase transitions have been attempted to be explained by evoking perturbations in magnetic degrees of freedom relevant to MnAs. In particular, Goodenough et al [14] explained the first-order 'H'-to-'O' transition in terms of a sharp change in the spin state of Mn atoms.

However, neutron scattering experiments showed that the magnetic moment of Mn atoms in MnAs does not change much in the 'O'-phase in comparison to the low-T 'H' phase [15,16] and, furthermore, the magnetic response of both the low-temperature 'H'- and elevated temperature 'O'-MnAs is characterized by FM correlations [17]. On the other hand, Bean and Rodbell proposed an alternative model where the exchange interaction is FM in both phases but, due to its strong dependence on the atomic volume, appears much smaller in the 'O' one, leading to zero net magnetization [18,19]. The model, however, is unable to explain the second-order transition at 400 K. It is unable to explain the metamagnetic phase transition either. In line with findings of EXAFS studies [20], more recent theoretical efforts suggested a phonon mediated mechanism for the first-order transition in MnAs [21,22], where an electron orbitals-specific competition between magnetic exchange and kinetic energies, including thermally activated local fluctuations of Mn spins, drive that transition [23]. However, the suggested structural fluctuations, in particular their magnitude and character, are not well established experimentally. Furthermore, a variety of properties of MnAs susceptible to local structure fluctuations, remain unexplained, including anomalous elastic properties [24,25] and a very low-thermal conductivity [26]. To fill the knowledge gap, we study the evolution of the average and local crystal structure of MnAs over a broad range of temperatures and magnetic fields by total x-ray scattering coupled to atomic pair distribution function (PDF) analysis. We find that the structural fluctuations in MnAs appear as anisotropic displacements of Mn atoms that emerge in the low-temperature "H" phase well below T_c, increase steeply at T_c, remain highly anisotropic in the 'O'- phase and finally disappear overwhelmed by trivial thermal excitations in the recovered 'H'-phase. The displacements can be viewed at as lattice degrees of freedom that bridge the different phases of MnAs, contributing to the observed peculiar evolution of its crystal structure and magnetic properties. Moreover, they appear susceptible to magnetic field, allowing us to induce distinct local structure states in MnAs at the same temperature, providing another evidence in support of our recent finding [27] that magnetic field and temperature are coupled but not necessarily equivalent control variables for triggering phase transitions in strongly correlated systems.

2. Experimental

2.1 Sample preparation and properties characterization. The sample was provided by American Elements as powder. Its magnetic properties were studied on a physical property measuring system (PPMS) from Quantum Design. Results are shown in Figure 1(*c*-*e*). In line with the findings of prior powder and single crystal studies [5, 9, 12,19], the ferromagnetic order in MnAs sharply disappears at T_c=318 K (Fig. 1*d*) but can be induced isothermally by applying a strong external field at a temperature just above T_c (Fig. 1*e*).

2.2 Synchrotron radiation studies. Synchrotron high-energy XRD experiments were conducted at the beamline 28-ID-1 at the National Synchrotron Light Source-II, Brookhaven National Laboratory using x-rays with energy of 74.46 keV (λ=0.1665Å). XRD data were collected while varying temperature between

220 K and 420 K, in steps of 3 K. Experimental XRD patterns and atomic PDFs derived from them using standard software [28] are summarized in Figure 2(*a-c*). High-energy XRD data were also obtained at a fixed temperature (320 K) slightly above T_c while applying an external magnetic field. Atomic PDFs derived from XRD data collected in magnetic field are summarized in Figure 2(*d*). More experimental details are given in Supplemental Material [29].

2.3 Average crystal structure as a function of temperature. To verify prior findings for the temperature evolution of the average crystal structure of MnAs and, at the same time, demonstrate the good quality of our experiment, high resolution XRD data were subjected to Rietveld analysis using the well-established software FullProf [30]. Representative Rietveld fits are shown in Figure S1(*a,c*) [29]. Rietveld refined lattice parameters and volume occupied by one MnAs formula unit are summarized in Figures 3(*a*) and 3(*b*), respectively. Well below T_c, the c_{hex} lattice parameter is seen to increase gradually with temperature whereas a_{hex} shrinks. In the temperature range from about 280 K to T_c, changes in the c_{hex} and a_{hex} accelerate and the atomic volume starts diminishing fast. In total, during the first-order transition, it drops by about 1.8 %. In the emerged 'O'-phase, the in-plane lattice parameters b_{ortho} and c_{ortho} and the orthogonal to them a_{ortho} parameter increase gradually with temperature. At the temperature of the second-order transition, b_{ortho} increases and c_{ortho} decreases by the same percentage whereas a_{ortho} does not change significantly. As a result, the atomic volume does not exhibit a noticeable discontinuity. In the recovered 'H'-phase, the lattice parameters and atomic volume of MnAs increase gradually with temperature. Overall, the results are fully consistent with the findings of prior studies [5,7,9,13-15], which attests to the good quality of our experiment.

2.4 Local atomic structure as a function of temperature As data in Figure 3(*a,b*) show, the crystal lattice in MnAs expands in some and shrinks in other directions with changing temperature, which is likely to result in local lattice distortions. To assess the distortions, the experimental PDFs were fit with structure models found plausible by Rietveld analysis, where the fits included interatomic distances within two unit cells of MnAs (~12 Å). Fits to longer interatomic distances reproduced the structure parameters derived by Rietveld analysis. The fits were performed using the well-established software PDFgui [31]. Representative PDF fits are shown in Fig. S1(*b,d*) [29]. PDF refined lattice parameters and atomic volume are compared with the results of Rietveld analysis in Figure 3(*a,b*). As can be seen in the Figure, Rietveld and PDF refined c_{hexa} lattice parameters and atomic volume for the low-temperature 'H'-phase differ systematically. In particular, locally, the latter appears diminished in comparison to the average structure. On the other hand, in the 'O'-phase, the PDF refined in-plane lattice parameter c_{ortho} appears systematically longer than the Rietveld refined c_{ortho}. The opposite is true for the b_{ortho} lattice parameter. The results indicate that, locally, atomic planes in MnAs suffer larger orthorhombic distortions in comparison to the average structure.

To reveal the local crystal structure in better detail, we computed first-neighbor Mn-Mn distances and summarized them in Figure 3(*c*). PDF refined models were used for the computations because, as defined and derived, atomic PDFs directly reflect interatomic distances. As can be seen in the Figure, both in-plane and interplane Mn-Mn distances change little in the temperature range from 220 K to 270 K. The changes accelerate between 270 K and T_c, where the interplane distance increases slightly and three distinct in-plane Mn-Mn distances emerge, reflecting the formation of zig-zag chains of Mn atoms in 'O'-MnAs (see Fig. 1*b*). The shortest and longest of these distances, respectively, increase and decrease with temperate upon further heating the sample. During the second-order phase transition taking place at 400 K, the three distinct in-plane Mn-Mn distances merge in a single one, reflecting the disappearing of Mn chains and recovering of the hexagonal symmetry in MnAs. First neighbor Mn-Mn distances in the recovered 'H'-MnAs are seen to change uniformly with temperature.

Mean-squared displacements of Mn atoms, U_{ij}, from their average position in the undistorted lattice, as computed from PDF fits, are shown in Figure 3(*d*). As can be seen in the Figure, both the in-plane and out-of-plane U_{ij} in low-temperature 'H'-MnAs gradually increase upon warming the sample to 270 K. When the temperature is increased further, the out-of-plane U_{ij} diminish whereas in-plane U_{ij} increase sharply. The observation indicates that, near T_c, the MnAs lattice dramatically softens in the Mn planes. Just above T_c, the out-of-plane U_{ij} increase whereas the in-plane U_{ij} drop and split into two branches, which include displacements along and orthogonal to the emerged Mn chains, respectively. The two branches merge into a single one when the temperature increases to about 350 K. At the second-order transition taking place at 400 K, the out-of-plane and in-plane U_{ij} decrease and increase sharply, respectively. In the high-temperature 'H' phase, Mn displacements are seen to increase gradually with temperature, i.e., appear determined by thermal excitation.

2.5 Average crystal structure as a function of magnetic field. To ascertain the less studied evolution of the average crystal structure with magnetic field, XRD data obtained at 320 K in magnetic field were subjected to Rietveld analysis. Representative Rietveld fits are shown in Figure S2(*a,b*) [29]. Rietveld refined lattice parameters are summarized in Figure 4(*a,b*). They are seen to change discontinuously at the critical magnetic field, H_c, where the initial 'O' phase becomes an 'H' phase through a metamagnetic transition. Furthermore, lattice parameters of the initial 'O' (Fig. 4*a*) and recovered 'O' phases (Fig. 4*b*) are not the same (e.g., a_{ortho} =5.719 Å in initial 'O'-MnAs vs a_{ortho} =5.729 Å in recovered 'O'-MnAs).

2.6 Local atomic structure as a function of magnetic field. Experimental PDFs obtained in magnetic field were fit with structure models found plausible by Rietveld analysis. Representative fits are shown in Fig. S2(*c,d*) [29]. PDF refined lattice parameters are compared with the results of Rietveld analysis in Figure 4(*a,b*). As can be seen in Figure 4(*a*), Rietveld and PDF refined lattice parameters in the low field ($< H_c$) treated 'O'-MnAs remain different with increasing field. The differences nearly disappear in the magnetic

field-induced ‘H’-phase (Figure 4*b*). Mean-squared displacements of Mn atoms, U_{ij}, as computed from the PDF fits, are shown in Figure 4(*c,d*). As expected, the two branches of the in-plane U_{ij} in the low field ($<H_c$) treated ‘O’-MnAs merge into a single branch in the magnetic-field-induced ‘H’-MnAs. Moreover, when ‘H’-MnAs emerges with increasing field, both the in-plane and out-of-plane U_{ij} decrease significantly. Their decreased value changes little when the field is brought back to zero and the ‘O’-phase is recovered. Evidently, not only the lattice parameters change from their initial values but also Mn positional disorder diminishes when MnAs is cycled in magnetic field, that is, using magnetic field, inaccessible by thermal treatment alone local structure states in MnAs can be induced.

3. Discussion

The exchange coupling between the magnetic moments of nearby Mn atoms in MnAs depends on their separation and includes contributions from interplane and in-plane Mn-Mn first neighbor interactions, which are ferromagnetic in low-temperature ‘H’-MnAs [23,32,33]. Theoretical studies have shown that the in-plane Mn-Mn first neighbor exchange interactions may become antiferromagnetic when Mn-Mn separations become comparable to the intrachain Mn-Mn distances in ‘O’-MnAs [23,33]. The currently accepted description of the temperature-driven ‘H’- to ‘O’-phase transition in MnAs envisages that, as temperature rises and Mn spin-flip fluctuations begin to set in, the ferromagnetic order weakens and, at T_c, it becomes energetically favorable for the MnAs structure to distort such that the crystal lattice symmetry is reduced to orthorhombic and short in-plane Mn-Mn bonds formed in the emerging zig-zag chains [23]. As our structural study shows, the crystal lattice of ‘H’-MnAs indeed exhibits highly anisotropic atomic displacements and local variations in the in-plane Mn-Mn distances well below T_c, e.g., starting at 270 K (see Fig. 3*c,d*). The displacements surge at T_c and then drop when temperature is increased further (Fig. 3*d*), following a “λ”-type temperature evolution characteristic to “soft-mode” type phase transitions [34]. It then may be that what drives the first-order transition is not merely the emergence of temperature driven spin-spin fluctuations but also a concurrent soft phonon mode type instability of the crystal lattice, involving a correlated, highly anisotropic in-plane displacement of Mn atoms toward one another to form stronger metallic bonds. With the temperature closely approaching T_c, due to the instability, Mn atoms would become increasingly displaced in a direction of the orthorhombic distortion, both reducing the crystallographic symmetry and leading to the emergence of Mn-Mn pairs separated at distances favoring AF exchange interactions and/or slightly reduced Mn magnetic moments, as predicted by DFT [23]. The increasing presence of magnetically inequivalent Mn-Mn pairs would amplify the temperature induced spin-spin fluctuations, leading to a frustration of the FM order and a magnetic state with zero net magnetization but non-zero Mn magnetic moments, as observed by experiment [15, 35]. Here is to be noted that although the structural phase transitions in MnAs are associated with the presence of an optical soft

mode, they are not ferroelectric in character because the mode is not at the center but at the M point of the Brillouin zone, i.e., is not polar [21, 22].

Based on the pioneering work of Guillaud [36] and temperature evolution of our magnetization data, it is tempting to speculate that had the displacements not been present, the magnetization would not have dropped to zero at 318 K but followed a Brillouin function-type decay and approached zero at a fictitious Curie temperature, T_C*, that is close to the temperature of the second-order transition taking place well above T_c. A Brillouin-type function fit to our magnetization data in the range from 5 K to 310 K produced a T_C* value of 370 K, as shown in Fig. 1*d* (red broken line). Depending on the particular data set and extrapolation details, values for T_C* have been found to vary between 360 K [32] to near 400 K [12, 36]. As our structure data show (Fig. 3*d*), T_C* appears near the temperature where the anisotropy in the in-plane U_{ij} of Mn atoms largely disappears because of increased thermal excitations effects, as demonstrated by the merging of the two branches of in-plane U_{ij} into one. That is, it appears that the emergence of highly anisotropic in-plane lattice displacements with increasing temperature destabilizes the low-temperature 'H' phase, stabilizes the 'O'-phase and destroys the FM order at T_c, which, otherwise, could have persisted to T_c^*. While the lattice parameters and atomic volume for 'O'-MnAs seem to evolve smoothly into those for recovered 'H'-MnAs with temperature (Fig. 3*a,b*), Mn U_{ij} are seen to change discontinuously (Fig. 3*d*) at 400 K, indicating that the second-order transition into a true PM phase involves abrupt changes in the local lattice distortions. The result highlights the importance of local lattice distortions in determining the magnetic properties of MnAs. Above 400 K, Mn U_{ij} are seen to evolve linearly with temperature, i.e. become largely thermal in character. The deviation of U_{ij} from the usual gradual increase with temperature, including their pronounced "λ"-shaped discontinuity extending between 270 K and T_c*, reflects the soft-mode lattice instability in MnAs [37-40]. The magnitude of the deviation, ΔU (Fig. 3*d*), may be viewed at as an amplitude of the mode. Signatures of a soft mode in MnAs that stabilizes its 'O'-phase have also been observed by time-resolved x-ray scattering on highly strained 70 nm MnAs/GaAs(001) thin films [41].

It may be expected that the presence of competing FM and AF exchange interactions between Mn magnetic moments in 'O'-MnAs just above T_c would make it easier for the higher-symmetry 'H'-phase to be recovered via a metamagnetic phase transition. In particular, when a strong enough magnetic field is applied, magnetic moments of Mn atoms would be pushed to align in a FM pattern, causing the atoms to re-position so that uniform in-plane Mn-Mn distances conducive to FM order are achieved. Concurrently, the crystal lattice symmetry would increase, and positional disorder of Mn atoms decrease as evidenced by the analysis of PDF data obtained in magnetic field (see Fig. 4*c,d*). The presence of highly anisotropic Mn U_{ij}, i.e. a pronounced soft lattice mode, is likely to be a major factor behind the rich pressure-magnetic phase diagram for MnAs observed by neutron diffraction, including helicoidal phases [42,43]. The presence

of intrinsic atomic positional disorder in MnAs may also well explain its extremely low thermal conductivity [24,25] and abnormal elastic properties near T_c [26].

4. Conclusion

Our variable temperature and magnetic fields study confirms the presence of a theoretically predicted [21,22] soft phonon mode in MnAs. It reveals that the mode is largely in-plane in character and involves a highly anisotropic displacement of Mn atoms with a mean-squared amplitude $\Delta U = 0.007$ Å^2 on top of the usual thermal displacements (~0.016 Å^2 ; see Fig. 3*d*). The mode appears in low-temperature 'H'-MnAs and persists in 'O"-MnAs, leading to an unusual decrease in the average lattice symmetry with increasing temperature. Other known examples of lowering of the average crystal symmetry upon heating through a first-order phase transition involving displacive atomic disorder include NaOH [44], La_2MgO_4 [45] and the structurally related superconducting $La_{1.85}Ba_{0.15}CuO_4$ [46]. Such large displacements would certainly modulate the exchange interactions and, together with temperature induced spin-spin fluctuations, frustrate the FM order. The emerged 'O'-phase incorporates fluctuating Mn-Mn distances and, hence, frustrated exchange interactions over a broad temperature range until thermal disorder overwhelms the in-plane anisotropy of the displacements and restores the higher symmetry 'H' phase. Last but not least, our study provides extra evidence that, although coupled, temperature and magnetic field are not necessarily equivalent variables for inducing transitions between competing phases in strongly correlated systems such as MnAs, where the lattice parameters, atomic volume and positional disorder in the resulting phase depend on which of the two is used to drive the system through the 'O'/'H' phase boundary.

Acknowledgments: This work was supported by the U.S. Department of Energy, Office of Science, Office of Basic Energy Sciences under Award No. DE-SC0021973 and used resources of the National Synchrotron Light Source at the Brookhaven National Laboratory provided by the DOE Office of Science under Contract No DE-SC0012704.

References:

[1] Hou Z, Li L, Liu C, Gao X, Ma Z, Zhou G, Peng Y, Yan Mi, Zhang X and Liu J 2021 Emergence of room temperature stable skyrmionic bubbles in the rare earth based $REMn_2Ge_2$ (RE = Ce, Pr, and Nd) magnets *Mat. Today Phys*. **17**, 100341

[2] Ma W, Xu X, Yin J-X, Yang H, Zhou H, Cheng Z, Huang Y, Qu Z, Wang F, Hasan M Z and Jia S 2021 Rare Earth Engineering in RMn_6Sn_6 (R=Gd-Tm, Lu) Topological Kagome Magnets *Phys. Rev. Lett*. **126**, 246602

[3] Gao C, Zeng Z, Peng S and Shuai C 2022 Magnetostrictive alloys: Promising materials for biomedical applications *Bioactive Mat*. **8**, 177

[4] Zuo S, Liu J, Qiao K, Zhang Y, Chen J, Su Na, Liu Y, Cao J, Zhao T, Wang J, Hu F, Sun J,

Jiang Ch and Shen B 2021 Spontaneous Topological Magnetic Transitions in $NdCo_5$ Rare-Earth Magnets *Adv. Mat*. **33**, 2103751
[5] Willis B. T. M. and Rooksby H P 1954 Magnetic Transitions and Structural Changes in Hexagonal Manganese Compounds *Proc. Phys. Soc. London* Sect. B **67**, 290
[6] Mosca D H, Vidal F, and Etgens V H 2008 Strain Engineering of the Magnetocaloric Effect in MnAs Epilayers *Phys. Rev. Lett*. **101**, 125503
[7] Wada H and Tanabe Y 2001 Giant magnetocaloric effect of $MnAs_{1-x}Sb_x$ *Appl. Phys. Lett*. **79**, 3302
[8] Franco V, Blazquez J S, Ipus J J, Law J Y, Moreno-Ramirez L M and Conde A 2018 Magnetocaloric effect: From materials research to refrigeration devices *Prog. Mat. Sci*. 93, 112
[9] Zieba A, Shapira Y and Foner S 1982 Magnetic phase diagram of MnAs: Effect of magnetic field on structural and magnetic transitions *Phys. Lett*. A **91**, 243
[10] Asadov S K, Zavadskii E A, Kamenev V I, Stefanovskii E P, Sukstanskii A L and Todris B M 2000 Relation of Magnetic and Structural Factors in the Course of Phase Transitions in MnAs-Based Alloys
Phys. Solid State Translation from Fizika Tverdogo Tela **42**, 1696
[11] Filatov S K 2011 General Concept of Increasing Crystal Symmetry with an Increase in Temperature *Cryst. Rep.* **56**, 953
[12] Mira J, Rivadulla F, Rivas J, Fondado A, Guidi T, Caciuffo R, Carsughi F, Radaelli P G and Goodenough J B 2003 Structural Transformation Induced by Magnetic Field and "Colossal-Like" Magnetoresistance Response above 313 K in MnAs *Phys. Rev. Lett*. **90**, 097203
[13] Menyuk N, Kafalas J A, Dwight K and Goodenough J B 1969 Effects of Pressure on the Magnetic Properties of MnAs *Phys. Rev*. **177**, 942
[14] Goodenough J B and Kafalas J A 1967 High-Pressure Study of the First-Order Phase Transition in MnAs *Phys. Rev*. **157**, 389
[15] Neumann K -U, Ziebeck K R A, Jewiss F, Daweritz L, Ploog K H and Murani A 2003 Magnetic correlations in the paramagnetic phases of MnAs *Physica B* **335**, 34
[16] Schwartz L H, Hall E L and Felcher G P 1971 Magnetic structure of MnAs and $MnAs_{0.92}P_{0.08}$ *J. Appl. Phys*. **42**, 1621
[17] Neumann K U, Dann S, Frohlich K, Murani A, Ouladdiaf B and Ziebeck K R A 2005 A Neutron Scattering Investigation of MnAs *Lect. Notes Phys*. **678**, 87
[18] Bean C P and Rodbell D S 1962 Magnetic Disorder as a First-Order Phase Transformation *Phys. Rev*. **126**, 104
[19] De Blois R W and Rodbell D S Magnetic first order phase transition in single crystal MnAs 1963 *Phys.Rev.***130**, 1347
[20] Palumbo O, Castellano C, Paolone A and Cantelli R 2005 Extended x-ray absorption fine structure study of the MnAs local structure at the phase transitions *J. Phys.: Condens. Matter* **17**, 1537
[21] Lazewski J, Piekarz P and Parlinski K Mechanism of the phase transitions in MnAs 2011 *Phys. Rev. B* **83**, 054108.
[22] Lazewski J, Piekarz P, Tobola J, Wiendlocha B, Jochym P T, Sternik M and Parlinski K Phonon mechanism of the magnetostructural phase transition in MnAs 2010 *Phys. Rev. Lett.* **104**, 147205
[23] Bocarsly J D, Johannes M D, Wilson S D and Seshadri R 2020 Magnetostructural coupling from competing magnetic and chemical bonding effects *Phys. Rev. Res*. **2**, 042048(R).
[24] Dorfler M and Barner K 1973 The elastic constants of MnAs *Phys. Stat. Sol*. A **17**, 141
[25] Barner K and Berg H 1978 Elastic anomalies at the second order phase transition in MnAs *Phys. Stat. Sol.* A**49**, 545

[26] Fujieda S, Hasegawa Y, Fujita A and Fukamichi K 2004 Thermal transport properties of magnetic refrigerants $La(Fe_xS_{1-x})_{13}$ and their hydrides, and $Gd_5Si_2Ge_2$ and MnAs *J. Appl. Phys*. **95**, 2429
[27] Petkov V, Rao T D, Abeykoon AM M, Galeano-Cabral J R and Wei K 2022 Spin-lattice coupling in magnetocaloric $Gd_5(Ge,Si)_4$ alloys by in situ x-ray pair distribution analysis in magnetic field *Phys. Rev. Mater.* **6**, 104407
[28] Juhás P, Davis T, Farrow C L and Billinge S J L 2013 *PDFgetX3*: a rapid and highly automatable program for processing powder diffraction data into total scattering pair distribution functions *J. Appl.Crystallogr*. **46**, 560
[29] Supplemental Material
[30] Rodriguez-Carvajal J 2001 Recent Developments of the Program FULLPROF *Commission on Powder Diffraction Newsletter* **26**, 12
[31] Farrow C L, Juhás P, Liu J W, Bryndin D, Božin E S, Bloch J, Proffen Th and Billinge S J L 2007 PDFfit2 and PDFgui: computer programs for studying nanostructure in crystals *J. Phys.: Condens. Matter* **19**, 335219
[32] Zieba A, Selte K, Kjekshus A and Andresen A F 1978 Phase Transitions in MnAs *Acta Chem. Scand. A* **32**, 173
[33] Rungger I and Sanvito S 2006 An ab initio study of the magnetostructural properties of MnAs *Phys. Rev. B*. **74**, 024429
[34] Nakanishi N, Nagasawa A and Murakami Y 1982 Lattice stability and soft modes *J. de Physique* **43**, C4-35
[35] Iikawa F, Brasil M J S P, Adriano C, Couto O D D, Giles C, Santos P V, Daweritz L, Rungger I and Sanvito S 2005 Lattice Distortion Effects on the Magnetostructural Phase Transition of MnAs *Phys. Rev. Lett.* **95**, 077203
[36] Guillaud G 1951 Les points de transformation des composés définis MnAs, MnBi en relation avec un mécanisme probable d'antiferromagnétisme J. De Phys. *Radium* **12**, 223
[37] Meissner G and Binder K 1975 Debye-Waller factor, compressibility sum rule, and central peak at structural phase transitions *Phys. Rev.* B **12**, 3948
[38] Rudin S P 2018 Generalization of soft phonon modes *Phys. Rev.* B **97**, 134114
[39] Venkataraman G 1979 Soft modes and structural phase transitions *Bull. Mater. Sci*. **1**, 129
[40] Jochym P T, Lazewski J and Szuszkiewicz W 2020 Phonon mode potential and its contribution to anharmonism *Sci. Rep*. **10**, 19783
[41] Vidal F, Zheng Y, Lounis L, Coelho L, Laulhé C, Spezzani C, Ciavardini A, Popescu H, Ferrari E, Allaria E, Ma J, Wang H, Zhao J, Chollet M, Seaberg M, Alonso-Mori R, Glownia J M, Eddrief M and Sacchi M 2019 Ultrafast Structural Dynamics along the β-γ Phase Transition Path in MnAs *Phys. Rev. Lett.* **122,** 145702
[42] Zou J D, Wada H, Shen B G, Sun J R and Li W 2008 Giant magnetocaloric effect and soft-mode magneto-structural phase transition in MnAs *Eur. Phys. Lett*. **81**, 4700
[43] Glazkov V P, Kozlenko D P, Podurets K M, Savenko B N and Somenkov V A 2003 Neutron diffraction investigation of the atomic and magnetic structures of MnAs at high pressures *Crystatallogr. Rep. Translation from Kristallografiya* **48**, 54
[44] Bleif H J and Dachs H 1982 Cystalline modifications and structural phase transitions of NaOH and NaOD *Acta Cryst.* **A38**, 470
[45] Tidey J P, Keegan Ch, Bristowe N C, Mostofi A A, Hong Z M, Chen B H, Chuang Y Ch, Chen W T and Senn M S 2022 Structural origins of the low-temperature orthorhombic to low-temperature tetragonal phase transition in high-Tc cuprates *Phys. Rev. B* **106**, 085112
[46] Paul D McK, Balakrishnan G, Bernhoeft N R, David W I F and Harrison W T A 1987 Anomalous Structural Behavior of the Superconducting Compound $La_{1.85}Ba_{0.15}CuO_4$ *Phys. Rev. Lett.* **58**, 1976

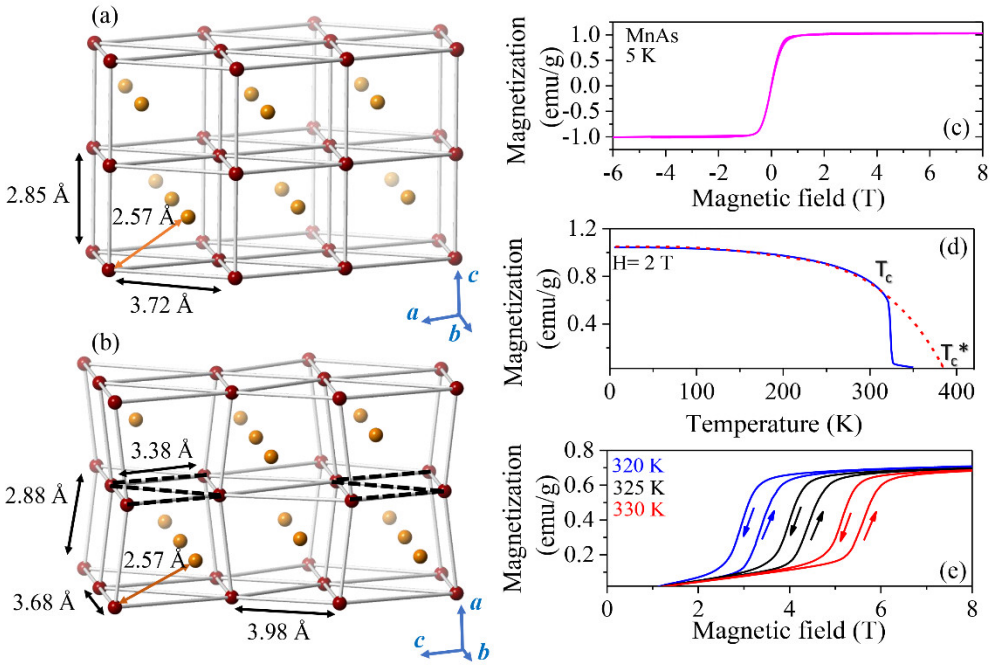

Figure 1. Fragments from the (*a*) 'H'- and (*b*) 'O'-crystal structure of MnAs, featuring alternating planes of Mn (brown circles) and As (yellow circles) layers. First neighbor Mn-As and Mn-Mn distances in both structures, including zig-zag chains in the 'O' phase (broken line) are also shown. (*c*) Magnetization of MnAs as a function of magnetic field (*c,e*) and temperature (*d*). The material exhibits a 1st order transition at T_c = 318 K. Broken red line in (*d*) is a Brillouin-type function extrapolation of the data to $T > T_c$ derived by a fit to the magnetization data in the range from 5 K to 310 K using a spin variable S=3/2, which is consistent with the experimental value for Mn magnetic moment of 3.3±0.1 μ_B found by neutron diffraction and 3.1±0.1 μ_B found by magnetization measurements [32]. The Brillouin function extrapolation crosses the temperature axes at a fictitious Curie temperature T_c* of 370 K. Data in (*e*) indicates the presence of a field induced metamagnetic transition. Arrows show the ascending and descending branches of the hysteresis curves.

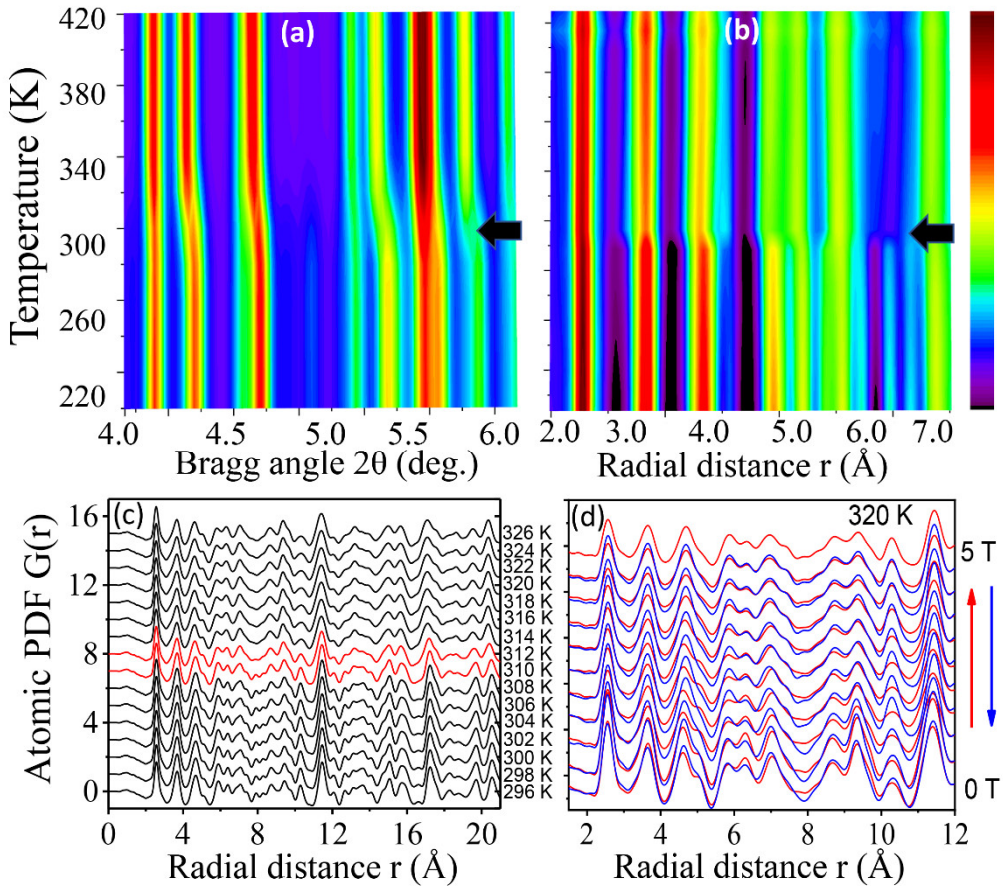

Figure 2. (*upper panel*) Synchrotron XRD patterns (*a*) and atomic PDFs (*b*) intensity color maps for MnAs. Arrows mark sharp structure changes taking place at 318 K. (*lower panel*) Evolution of atomic PDFs for MnAs as a function of temperature. (*c*) The PDFs in the immediate vicinity of T_c are highlighted in red. Evolution of atomic PDFs as a function of external magnetic field (*d*) measured at 320 K, where MnAs undergoes a metamagnetic phase transition. PDF data are seen to exhibit a strong hysteresis effect. The intensity of XRD and PDF peaks increases as their color changes from blue towards dark red. The increase is at a constant rate, as indicated by the color bar on the right side of plot (*b*).

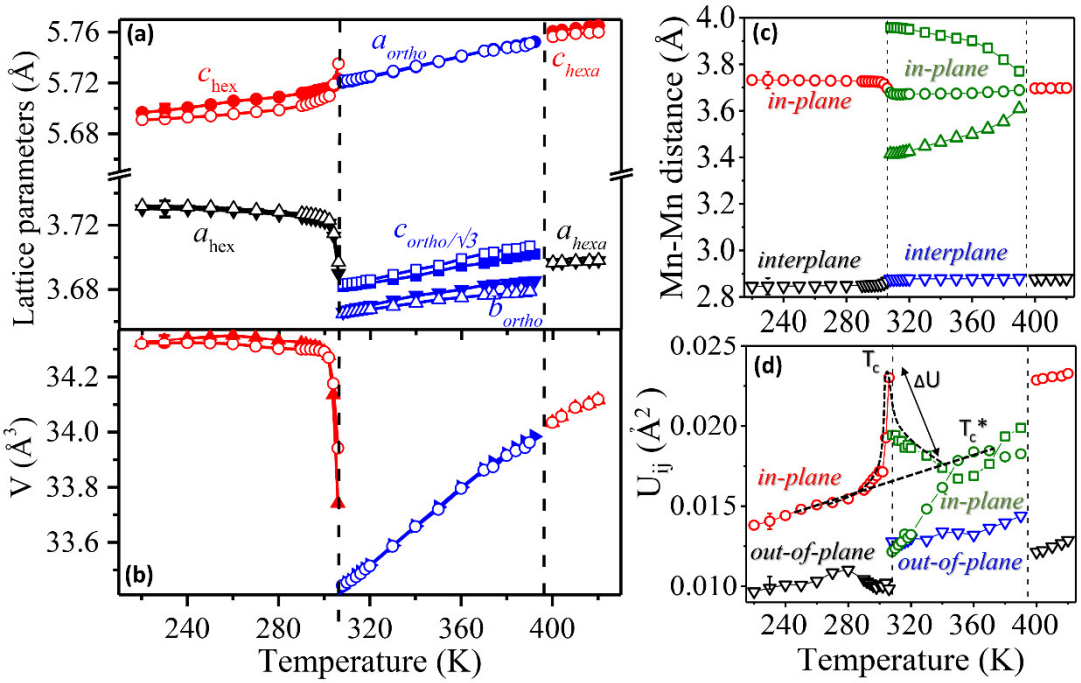

Figure 3. (*a,b*) Rietveld (solid symbols) and PDF (open symbols) refined lattice parameters and atomic volume, V, in 'H'- and 'O'-MnAs. Both change sharply at T_c=318 K. The change taking place at the second-order transition (~400 K) is much less sharp. Data for b_{ortho} and $c_{ortho/\sqrt{3}}$ are given, respectively, as triangles and squares whereas data for c_{hex} and a_{ortho} are given as circles. (*c*) In-plane and interplane Mn-Mn distances in MnAs derived from PDF refined structure models. The in-plane distances change sharply at both phase transitions whereas changes in the interplane distances are gradual. (*d*) Also shown are mean-square displacements of Mn atoms, U_{ij}, derived from PDF fits. The displacements change sharply at both phase transitions. Particularly strong is the "λ-type" divergence of the in-plane displacements (black broken line) taking place at T_c. In the 'O'-structure, Mn displacements along and orthogonal to the chains are given as green circles and squares, respectively. ΔU is the amplitude of mean squared displacements on top of the usual thermal displacements (inclined broken line). Vertical broken lines mark the first and second order transitions. The fictitious Curie temperature, T_c*, is also shown. Error bars are very close to the size of used symbols.

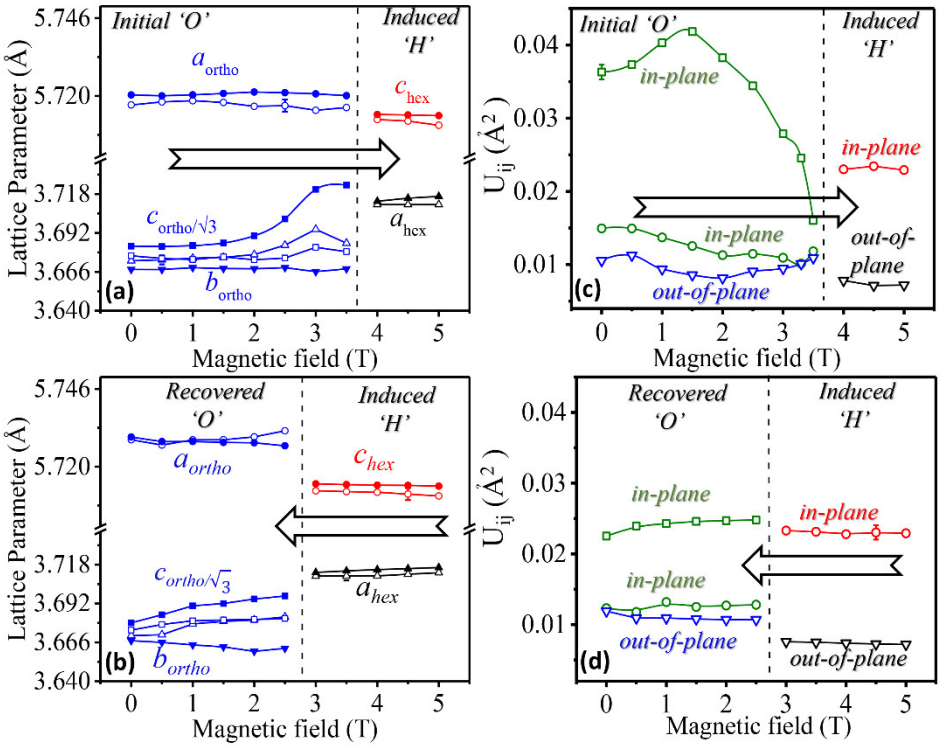

Figure 4. (*a,b*) Evolution of Rietveld (solid symbols) and PDF (open symbols) refined lattice parameters at 320 K with increasing and decreasing magnetic field. Data for b_{ortho} and $c_{ortho/\sqrt{3}}$ are given, respectively, as triangles and squares whereas data for c_{hex} and a_{ortho} are given as circles. (*c,d*) Evolution of in-plane and out-of-plane mean-square displacements of Mn atoms, U_{ij}, with increasing and decreasing magnetic field. In the initial and recovered 'O' phase, the in-plane Mn displacements along and orthogonal to Mn-Mn chains are given as green circles and squares, respectively. Lattice parameters and U_{ij} are seen to change sharply at the critical magnetic field H_c (vertical broken line), where the material undergoes a first order metamagnetic transition. Significant hysteresis effects are also seen, including differences between the lattice parameters and Mn displacements in the initial and recovered 'O'-MnAs. Error bars are every close to the size of used symbols.

Supplemental Materials

Lattice instability and magnetic phase transitions in strongly correlated MnAs

Valeri Petkov[1], Adeel Zafar[1], Durga R. Tadisetti[1,2] and Milinda AM Abeykoon[3]

[1]*Department of Physics, Central Michigan University, Mt. Pleasant, Michigan 48858, USA*
[2]*Department of Physics, GITAM, Visakhapatnam, Andhra Pradesh 53004, India*
[3]*Photon Sciences Division, Brookhaven National Laboratory, Upton, New York 11973, USA*

Synchrotron high-energy XRD experiments: The experiments were conducted at the beamline 28-ID-1 (PDF) at the National Synchrotron Light Source-II, Brookhaven National Laboratory using x-rays with energy of 74.46 keV (λ=0.1665Å). The powder sample was tightly packed and sealed in a Kapton tube and positioned inside a liquid He cryostat used to control its temperature. X-ray diffraction data were collected in transmission geometry using an amorphous silicon PerkinElmer area detector while varying temperature between 220 K and 420 K, in steps of 3 K. Two data sets were obtained at each temperature point. One of the data sets was obtained with the detector positioned 204 mm away from the sample to reach high wave vectors, q, (q_{max}=28 $Å^{-1}$ in the current experiment) necessary to obtain high real space resolution atomic PDFs. The PDFs were derived from the XRD data using a well-established protocol [S1]. The other data set was obtained with the detector positioned 1000 mm away from the sample to achieve high resolution in reciprocal space necessary for Rietveld analysis described below. Experimental XRD patterns and atomic PDFs obtained at different temperatures are summarized in Figure 2 in terms of intensity color maps. The patterns and PDFs are seen to undergo sharp changes where, according to the independently collected magnetic data (Fig. 1d), the magnetization sharply drops to zero, confirming the presence of a concurrent structural and magnetic phase transition in MnAs. The changes in the local crystal structure taking place during the first-order hexagonal to orthorhombic transition, as reflected by experimental atomic PDFs, are highlighted in Figure 3(c). No sharp changes are seen in the vicinity of the second-order orthorhombic to hexagonal phase transition taking place at about 400 K. High-energy XRD data were also obtained at a fixed temperature (320 K) slightly above T_c (318 K) while applying an external magnetic field with a strength of up to 5 T. Because of experimental constraints related to the combined use of an electromagnet and cryostat, this time x-rays with energy of 116.63 keV (λ=0.1063 Å) were used. Atomic PDFs derived from diffraction data collected in magnetic field are summarized in Figure 3(d). As can be seen in the Figure, the PDFs exhibit significant hysteresis effects.

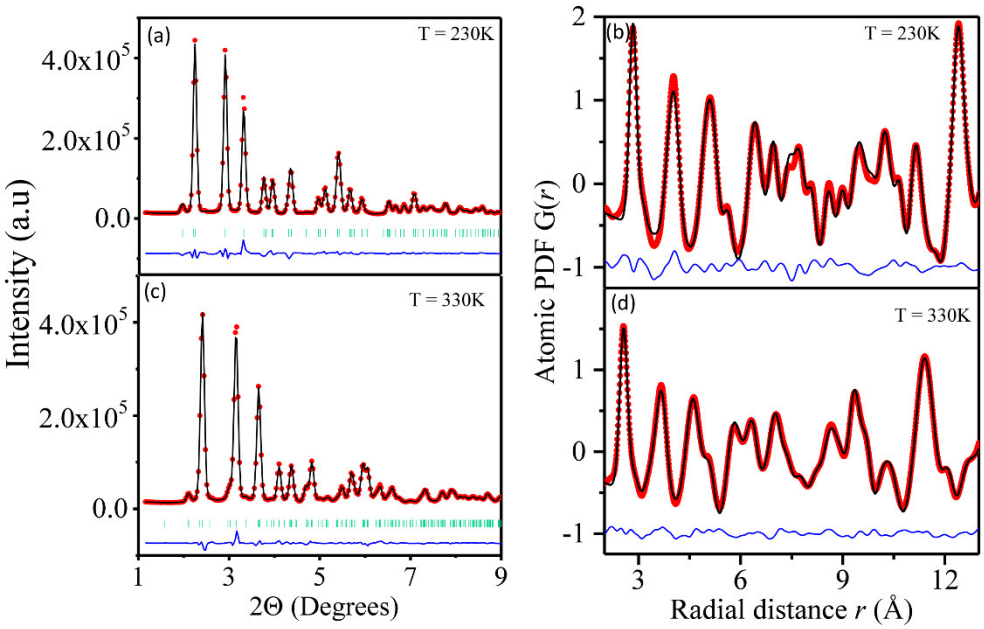

Figure S1. (a,c) Rietveld fits (black line) to XRD patterns (red dots) for MnAs taken at 230 K and 330 K, where the material adopts a hexagonal and orthorhombic crystal structure, respectively. Positions of Bragg peaks are given as green bars and the residual difference is given as a blue line. The goodness-of-fit indicator, R_{wp}, for both fits is close to 6%. (b,d) Fits (black line) to PDFs (red dots) for MnAs obtained from the respective XRD patterns shown on the left. The residual difference is given as a blue line. The goodness-of-fit indicator, R_{wp}, for both fits is close to 12 %. Note that, usually, R_{wp} for PDF fits appears larger than R_{wp} for Rietveld fits. The reason is that XRD patterns being fit take into account Bragg scattering alone whereas PDFs take into account both the Bragg and diffuse components of the XRD patterns. This does not diminish its usefulness as a quantity guiding PDF fits and allowing us to discriminate between competing structure models.

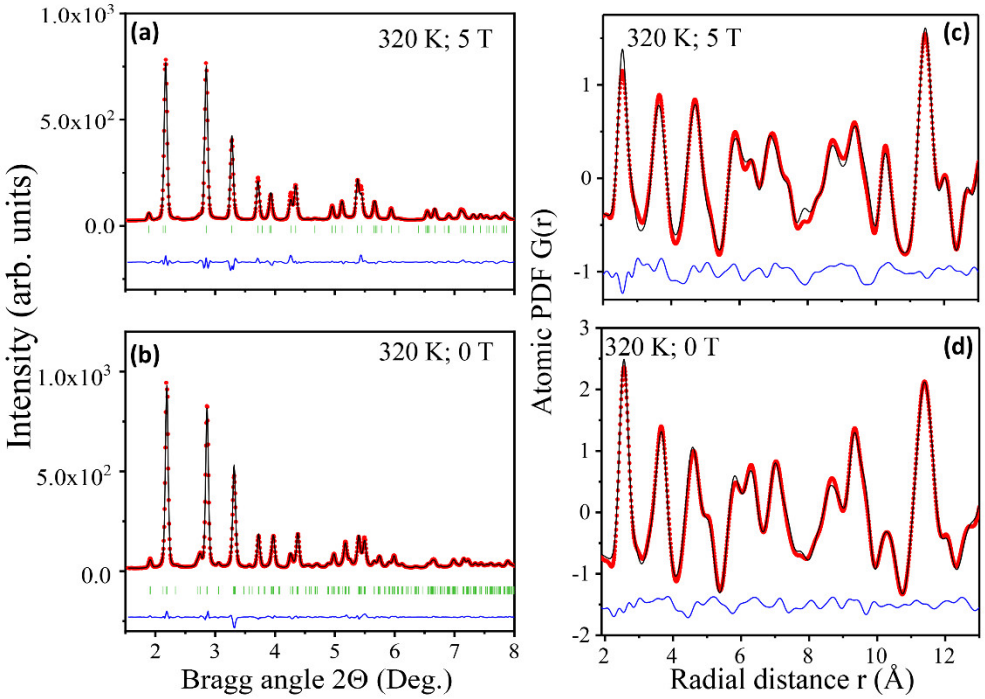

Figure S2. (a,b) Rietveld fits (black line) to XRD patterns (red dots) for MnAs taken at a constant temperature of 320 K, i.e. above T_c, once in zero magnetic field and a second time in a field of 5 T, where the material adopts an orthorhombic and hexagonal structure, respectively. Positions of Bragg peaks are given as green bars and the residual difference is given as a blue line. The goodness-of-fit indicator, R_{wp}, for both fits is close to 6%. (c,d) Fits (black line) to PDFs (red dots) for MnAs obtained from the respective XRD patterns shown on the left. The residual difference is given as a blue line. The goodness-of-fit indicator, R_{wp}, for both fits is close to 12 %, i.e. pretty good. %. Note that, usually, R_{wp} for PDF fits appears larger than R_{wp} for Rietveld fits. The reason is that XRD patterns being fit take into account Bragg scattering alone whereas PDFs take into account both the Bragg and diffuse components of the XRD patterns. This does not diminish its usefulness as a quantity guiding PDF fits and allowing us to discriminate between competing structure models.

References

S1. Juhás P, Davis T, Farrow C L and Billinge S J L 2013 PDFgetX3: a rapid and highly automatable program for processing powder diffraction data into total scattering pair distribution functions J. *Appl. Crystallogr*. **46**, 560